Breaking the Meyer-Overton Rule: Predicted Effects of Varying Stiffness and Interfacial Activity on the Intrinsic Potency of Anesthetics

Robert S. Cantor
Department of Chemistry, Dartmouth College, Hanover, New Hampshire 03755 USA

ABSTRACT Exceptions to the Meyer-Overton rule are commonly cited as evidence against indirect, membrane-mediated mechanisms of general anesthesia. However, another interpretation is possible within the context of an indirect mechanism in which solubilization of an anesthetic in the membrane causes a redistribution of lateral pressures in the membrane, which in turn shifts the conformational equilibrium of membrane proteins such as ligand-gated ion channels. It is suggested that compounds of different stiffness and interfacial activity have different intrinsic potencies, i.e., they cause widely different redistributions of the pressure profile (and thus different effects on protein conformational equilibria) per unit concentration of the compound in the membrane. Calculations incorporating the greater stiffness of perfluoromethylenic chains and the large interfacial attraction of hydroxyl groups predict the higher intrinsic potency of short alkanols than alkanes, the cutoffs in potency of alkanes and alkanols and the much shorter cutoffs for their perfluorinated analogues. Both effects, increased stiffness and interfacial activity, are present in unsaturated hydrocarbon solutes, and the intrinsic potencies are predicted to depend on the magnitude of both effects and on the number and locations of multiple bonds within the molecule. Most importantly, the intrinsic potencies of polymeric alkanols with regularly spaced hydroxyl groups are predicted to *rise* with increasing chain length, without cutoff; such molecules should serve to distinguish unambiguously between indirect mechanisms and direct binding mechanisms of anesthesia.

INTRODUCTION

The potency of a general anesthetic is usually described by its concentration in the phase in which it is administered (gas or aqueous); the lower the concentration, the higher the potency. A century ago, Overton (1901, translation 1990) and Meyer (1899, 1901) independently discovered that for many compounds the anesthetic potency (as measured by the inverse of its aqueous phase molar concentration c_w^*) is nearly linearly correlated with its oil/water partition coefficient $K_{o/w} = c_o/c_w$, where c_o and c_w represent relative equilibrium concentrations of the anesthetic in the oil and water phases, respectively. There is a thermodynamically equivalent correlation between the oil/gas partition coefficient $K_{o/g} = c_o/c_g$ of the anesthetic and its potency measured by the inverse of its gas phase concentration c_g^*. The correlation is remarkably good over a wide range of anesthetics, using olive oil as the oil phase, as in the original work of Meyer and Overton, and improves considerably in both the quality of the correlation and the increased range of anesthetics if bulk octanol (Franks and Lieb, 1978) or a fully hydrated fluid lipid bilayer (Janoff et al., 1981; Taheri et al., 1991; Vaes et al., 1997; Meijer et al., 1999) is used as the "oil" phase. To the extent that anesthetics obey this Meyer-Overton correlation, the anesthetic concentration in the oil phase, $c_o^* = K_{o/g}\, c_g^* = K_{o/w}\, c_w^*$, will be constant. If the oil is a lipid bilayer, then c_o^* represents the molar concentration of anesthetic in the bilayer, which indicates that anesthetic potency is determined by the bilayer concentration of anesthetic, independent of its molecular identity. As was realized long ago, this correlation strongly suggests an indirect mechanism of anesthesia in which the activity of the membrane protein(s) responsible for anesthesia is modulated by variations in some crucial property of the membrane, which is perturbed by the incorporation of an anesthetic solute to a degree determined by its concentration in the bilayer.

In the context of an indirect mechanism, it is natural to define an intrinsic potency as inversely proportional to the membrane concentration of anesthetic, which would be expected to vary little among anesthetics that closely follow the Meyer-Overton rule. The apparent potency for such compounds, inversely proportional to c_g^* (or c_w^*) may vary widely, but $K_{o/g}$ (or $K_{o/w}$) varies in inverse proportion so as to keep the intrinsic potency roughly constant. The concentrations in lipid bilayers of many such anesthetics can be determined from measured partial pressures or aqueous concentrations and bilayer/water or bilayer/gas partition coefficients (Janoff et al., 1981; Taheri et al., 1991; Vaes et al., 1997; Meijer et al., 1999). For pure lipid bilayers such as dimyristoylphosphatidylcholine (DMPC), the clinically relevant mole fraction of anesthetics in the lipid bilayer is roughly $x^* = 0.02$ to 0.05 for anesthetics that obey the Meyer-Overton rule (Janoff and Miller, 1982), although the value decreases considerably if cholesterol is incorporated in the bilayer (Miller, 1985; Franks and Lieb, 1986). Clearly, the "typical" value of x^* will depend on the choice of anesthetic endpoint, the molecular composition of the bilayer, etc., so this range of values of x^* provides only a rough estimate.

It is not surprising that the exceptions to this rule have received much attention. For example, short chain 1-al-

Received for publication 14 August 2000 and in final form 5 February 2001.

Address reprint requests to Robert S. Cantor, Department of Chemistry, Dartmouth College, Hanover, NH 03755. Tel.: 603-646-2504; Fax: 603-646-3946; E-mail: rcantor@dartmouth.edu.

0006-3495/01/05/2284/14 $2.00

kanols have somewhat greater intrinsic potency than the rule would predict (Fang et al., 1997). However, as their chain length n increases, the intrinsic potency decreases (x^* increases) up to $n \approx 12$, beyond which the alkanols have no potency, i.e., the homologous series exhibits a cutoff (Pringle et al., 1981; Franks and Lieb, 1986). Within this series, $K_{o/g}$ (or $K_{o/w}$) increases very rapidly with increasing chain length (by a multiplicative factor of approximately 3 per added methylene group.) Thus, the gradual decrease in intrinsic potency occurs simultaneously with an increase in apparent potency for this series, resulting in a cutoff that is abrupt only for the apparent potency. This behavior is observed for other homologous series. For example, for α,ω-alkanediols, a decrease in intrinsic potency occurs with increasing chain length, but less rapidly than for alkanols (Moss et al., 1991). Alkanes, which are much less potent than the rule would predict even when short, further lose intrinsic potency with increasing chain length, with a cutoff at shorter length than for alkanols (Liu et al., 1993, 1994b). Perfluorinated alkanes and perfluoroalkyl methanols of the form $C_{n-1}F_{2n-1}CH_2OH$ also exhibit a cutoff, but at even shorter chain lengths (Pringle et al., 1981; Liu et al., 1994a; Eger et al., 1994, 1999a).

Deviations from the Meyer-Overton rule can be interpreted in various ways. Most commonly, they are presented as evidence that the fundamental premise of an indirect mechanism is incorrect, and that anesthetics therefore are more likely to act by binding directly to protein sites (Krasowski and Harrison, 1999; Franks and Lieb, 1994), although the direct experimental evidence for the location of such sites on ligand-gated ion channels is sparse (Eckenhoff and Johansson, 1997; Pratt et al., 2000; Mascia et al., 2000). However, there are other interpretations. The most obvious one is that an anesthetic mechanism may indeed be membrane-mediated, but those solutes that disobey the rule have different intrinsic potencies. In other words, the effect of solutes on that property of the bilayer that alters protein conformational equilibria depends not only on membrane concentration but also on the identity of the solute. What property of the membrane is altered upon incorporation of anesthetics but not by nonanesthetics, is mechanistically linked to protein conformational equilibria, and causes significant shifts in protein equilibria at clinically relevant anesthetic concentrations?

Various bilayer properties have been considered as a possible link between changes in bilayer composition and resulting modulations in the activity of key intrinsic membrane proteins. As discussed previously (Cantor, 1999a,c), membrane characteristics such as hydrophobic thickness, dipole potential, fluidity, curvature elastic properties, proximity to phase transitions, and the degree of lateral microheterogeneity all vary with membrane composition and have thus been suggested as having a potentially strong influence on membrane protein function (Brown, 1997; deKruijff, 1997; Epand, 1996; Gruner, 1991; Hui, 1997; Lundbaek and Andersen, 1999; Morein et al., 1996; Mouritsen and Jørgensen, 1997; Mouritsen and Bloom, 1993; Nielsen et al., 1998; North and Cafiso, 1997; Qin et al., 1995). However, it has been noted (Franks and Lieb, 1994) that the changes in most of these properties (thickness, order parameter profiles, phase transition temperatures) are very small at clinically relevant concentrations of anesthetics and can be produced in the absence of anesthetic through slight changes in other variables, such as temperature. [It is important to note that the increase in gas-phase, but not aqueous-phase, apparent potencies with decreasing temperature of most inhalation anesthetics is accompanied by an increase in oil/gas partition coefficients (Franks and Lieb, 1982) such that the clinically relevant membrane concentration x^* does not depend sensitively on temperature. Thus, a plausible indirect mechanism would require a bilayer property that is strongly affected by anesthetics but only weakly by temperature changes.] Were there no bilayer properties both sensitive to incorporation of solutes and capable of influencing protein equilibria, it could be concluded that such indirect mechanisms are likely to play at most a minor role in the modulation of protein activity. However, it has been suggested (Gruner, 1991; Seddon and Templer, 1995; Cantor, 1998, 1999a) that the distribution of lateral stresses (i.e., the lateral pressure profile) in bilayers may be such a property, because it is predicted (Cantor, 1998, 1999a) to be strongly affected by incorporation of interfacially active solutes as well as by altered lipid composition, but not by small changes in temperature; more importantly, it is mechanistically linked to altered protein conformational equilibria.

A stringent test of an indirect mechanism involving the lateral pressure profile is, then, to determine whether it accurately predicts the known anomalies in the Meyer-Overton correlation. So, in the present paper, statistical thermodynamic calculations are used to predict the intrinsic potencies and thus the existence of cutoffs among the series of alkanes, alkanols, α,ω-alkanediols, and their stiffer perfluorinated counterparts, which can be compared to experimental results, at least qualitatively. Predictions are also reported for classes of molecules for which potencies have not yet been measured. In particular, the intrinsic potency of oligomeric alkanols (i.e., alkanols with regularly spaced hydroxyl groups) is predicted to increase roughly linearly with the number of repeat units in the oligomer, and thus with chain length. Because it would appear difficult for such increasingly large molecules to be accommodated in any binding site (no matter how nonspecific), a measurement of the potencies of such molecules would be expected to distinguish unambiguously between indirect and direct binding mechanisms of anesthesia.

THEORY

An indirect mechanism: the lateral pressure profile

As discussed in detail elsewhere (Cantor, 1999a,b), a lipid bilayer is characterized by very large lateral pressure den-

sities $p(z)$ distributed nonuniformly (i.e., varying with depth z) in the hydrophobic interior, balanced largely by tensions (negative pressures) at the aqueous interfaces (Israelachvili et al., 1980; Seddon, 1990; Xiang and Anderson, 1994; Seddon and Templer, 1995; Ben-Shaul, 1995; Harris and Ben-Shaul, 1997; Venturoli and Smit, 1999; Lindahl and Edholm, 2000). Transmembrane domains of proteins such as ligand-gated ion channels are necessarily subjected to these lateral pressures. A conformational transition of a membrane protein such as the opening of an ion channel results in a change in shape that will, in general, be characterized by a lateral expansion or contraction that varies with depth in the membrane, i.e., a nonuniform change in protein cross-sectional area in the transmembrane domain $\Delta A(z)$. Because the bilayer exerts lateral pressures against which the protein expands or contracts laterally, this transition involves mechanical work, the amount determined by the depth dependence of the lateral pressure profile and of the changes in protein cross-sectional area. A change in membrane composition, such as the incorporation of hydrophobic or amphiphilic solutes, is predicted (Cantor, 1998, 1999a) to cause a significant depth-dependent redistribution of these lateral pressures $\Delta p(z)$, resulting in a shift in the protein conformational equilibrium and thus in altered sensitivity of the protein to its normal agonist.

Unfortunately, there exists little direct experimental information on the change in shape of the transmembrane domains of postsynaptic ligand-gated ion channel proteins that accompanies the conformational transition (channel opening) relevant to their function. Still, there is considerable evidence (Popot and Engelman, 2000, and references therein) suggesting that the transmembrane domains of many intrinsic membrane proteins comprise bundles of predominantly α-helical secondary structural units that span the bilayer, and that for such bundles, the protein may achieve its conformational change with a relatively small expenditure of free energy through a cooperative reorientation of the transmembrane segments of the bundle, as has been reported for the nicotinic acetylcholine receptor (Unwin, 1993, 1995). In recent work (Cantor, 1999b), such collective reorientations have been analyzed using simple geometric models of collective tilts and rotations of bundles of both kinked and cylindrical helices, and it is shown that such conformational changes are particularly sensitive to redistributions of membrane lateral pressures. More precisely, it is readily shown (Cantor, 1999b) that at this level of approximation, the shifts in protein conformational equilibria depend predominantly on changes in the first and second integral moments of the pressure distribution. For symmetric bilayers, the first moment can be expressed as

$$\Delta P_1 = \int_0^h z\Delta p(z)\mathrm{d}z \qquad (1)$$

where $z = 0$ at the center of the bilayer and $z = -h$ and h at the aqueous interfaces. In essence, ΔP_1 is a measure of a shift in the center of the lateral stress distribution in each leaflet of the bilayer away from ($\Delta P_1 > 0$) or toward ($\Delta P_1 < 0$) the center of the bilayer. (The interpretation of the second moment ΔP_2 is more complex, but since the trends for ΔP_2 and ΔP_1 are predicted to be similar, only the results for ΔP_1 are discussed below.) Using these geometric models, the magnitude of ΔP_1 required to generate a significant change in protein conformational equilibrium can be estimated (Cantor, 1999b). For example, it is shown that for a protein of radius ~20 Å that undergoes a small tilt/rotation of order 5° to 10°, a shift in conformational equilibrium by a factor of two would be predicted for $|\Delta P_1|$ of order 0.02 (in units of k_BT Å^{-1}), the direction of the equilibrium shift determined by the sign of ΔP_1. If the mole fraction of solute in the bilayer is denoted x, then the intrinsic potency of an anesthetic can be defined as $S = \Delta P_1/x$. Taking $x^* \approx 0.02$ to 0.05 as a rough estimate (Janoff and Miller, 1982) of the mole fraction of an anesthetic (one that follows the Meyer-Overton correlation, as discussed earlier) in the bilayer at its EC_{50} concentration (i.e., at c_w^*), then $S \approx 0.5\ k_BT$ Å^{-1} provides an order of magnitude estimate of the intrinsic potency of anesthetics that obey the Meyer-Overton rule. Those molecules with anomalously low intrinsic potencies will have smaller values of S. Molecules predicted to have $S \approx 0$ would be nonanesthetics in the sense that they would not cause anesthesia at any membrane concentration, and would be predicted to have no effect on the anesthetic potency of standard anesthetics, as measured through additivity studies. Those solutes predicted to have $S < 0$ would have negative anesthetic potency, in the sense that they would be predicted to decrease the potency (i.e., increase the EC_{50} or MAC) of standard anesthetics in additivity studies, the magnitude of the effect increasing with the magnitude of S.

CALCULATION METHODOLOGY

Mean-field statistical thermodynamic theory is used to calculate the equilibrium properties of the lipid bilayer system, using a modified lattice model to describe the chain conformational contributions to the free energy. Except as discussed below, the approach is essentially identical to that used in recent work (Cantor, 1999a) to predict pressure profiles for bilayers for a wide range of lipid and lipid/solute compositions. A summary of the method and approximations is provided here; the interested reader should refer to Cantor (1999a) and references therein for details. The power of this kind of methodology for predicting structural and thermodynamic properties has been shown for aggregates of surfactants in solution, and for self-assembled or spread monolayer and bilayer films (Ben-Shaul, 1995; Ben-Shaul and Gelbart, 1994; Leermakers and Lyklema, 1992; Wijmans et al., 1994; Leermakers and Scheutjens, 1988; Cantor, 1995, 1996). As with all models, it relies on assumptions and approximations that serve to make the calculations tractable and result in interpretable predictions. The bilayer is treated as two compact monolayers, in each of which the segments of the acyl chains occupy space at constant bulk density, i.e., no free volume is permitted. The distribution of chain segments is described using a lattice model, in which a chain configuration is defined as occupying a particular

set of contiguous lattice sites. As in previous work, the boundary between the hydrophilic (head group) region and hydrophobic interior of the bilayer is approximated by a sharp planar interface. For the lipids, the junction of each acyl chain with its head group is constrained to reside on that plane, so that, for example, the complexity of the glycerol/carbonyl linkage between the phosphocholine head group and the acyl tails in phospholipids is completely ignored, as is the considerable roughness present in the interfacial region (Merz and Roux, 1996; Tielemann et al., 1997). Although interfacial roughness could readily be incorporated into the model (Leermakers and Scheutjens, 1988), it would require assumptions about additional interaction energies that are not well known, so it is unlikely that any additional predictive value would result. For purposes of describing hydrophobic solutes, the calculation of the conformational free energy has been modified and extended in the present work to allow all possible locations of the solute in the bilayer. For simplicity of calculation, neither lipid nor solute chains are allowed to cross the bilayer midplane, i.e., there is no interdigitation between monolayers. This restriction certainly causes an increase in the fraction of bonds oriented horizontally near the midplane, affecting the orientational ordering and the lateral pressure in that region. However, for most biological membranes there is little interdigitation, so this approximation is expected to be of minor importance.

The bilayer free energy contains both entropic and energetic contributions. The configurational entropy of the lipid and solute chains is calculated in mean-field approximation, incorporating bond-correlated excluded volume of chain segments. Three contributions to the internal energy of the bilayer are incorporated: segmental energies (including bending stiffness and, as appropriate, a local attraction of selected segments for the aqueous interface), interfacial tension, and head group interactions. At discrete values of the lipid surface density (at which the membrane thickness is an integer multiple of the size of a lattice site), the free energy is minimized with respect to the probability distribution of chain conformations, subject to the constraints of constant bulk density (one chain segment per lattice site) within the hydrophobic core of the bilayer, from which the depth-dependent pressures (and the total lateral pressure) are obtained. The calculated free energy values are fit to a polynomial in the surface density, the minimum of which determines the equilibrium surface density and the lateral pressure profile.

For both lipid and solute molecules, the lattice statistical mechanical approach provides the equilibrium probability distribution $P(q)$ of chain conformational states q, from which conformational averages such as the spatial distribution of chain segments can be determined. For a solute of chain length n, a conformational state q is defined by the set of sites occupied by its n segments, each of which is defined by its depth z in the membrane (as well as the spatial direction of its bonds to the adjacent segments on the chain.) For a given solute conformation q, we let $\phi_q(z)$ represent the total number of segments of the solute at depth z in the lattice (irrespective of the directional orientations of the bonds to adjacent segments on the chain.) On average, the number of solute segments at depth z is given by $\phi(z) = \Sigma_q P(q)\ \phi_q(z)$. Since each solute chain has n segments, the spatial probability distribution of solute segments, i.e., the fraction of solute segments found in a layer of lattice sites at depth z, is $\psi(z) = \phi(z)/n$.

Solute and lipid characteristics

Solute: chain stiffness

In unsubstituted, saturated alkanes, the hydrocarbon chain is semiflexible, whereas for some substituted alkanes, and at sites of unsaturation (alkenes and alkynes) the molecule can become considerably more rigid. In particular, for perfluorinated alkanes, the energetic cost for local bending of the chain is considerably greater than for alkanes. Also, detailed calculations (Smith et al., 1994) indicate that the distribution of conformational states of perfluorinated alkanes is more complex than for alkanes. The effective gauche/trans energy difference is roughly twice that of alkanes, with a large additional energy cost for adjacent gauche conformers, resulting in a reduction in the probability ω of a chain bend by roughly a factor of three compared to alkanes. In the lattice model used in the calculations, we thus estimate $\omega[(CF_2)_x] \approx 0.15$, with $\omega[(CH_2)_x] = \omega_{flex} \approx 0.45$ as in prior work (Cantor, 1999a). For simplicity, these values are taken to be independent of the substituents on the adjacent segments. Note that in chain molecules of n segments, the stiffness is only defined for the $n - 2$ interior segments, i.e., at segments $i = 2, 3, \ldots, n - 1$.

For the triple bonds in alkynes, the increase in rod-like stiffness at each of the (interior) carbons is very high. In alkenes, both *trans* and *cis* isomers are more rigid, but the backbone of the *trans* isomer is better modeled as more extended than that of saturated alkanes ($\omega_{rod} < \omega_{flex}$), whereas *cis* isomers are stiffly bent ($\omega_{bent} \gg 1$). If the local rigidity at internal segments i is denoted r_i, with $r_i = s$ (rod-like, ω_{rod}), f (semiflexible, ω_{flex}), or b (bent, ω_{bent}) then the distribution of molecular rigidity along the solute chain can be expressed as $\{r_2, r_3, \ldots, r_{n-1}\}$. An unsaturated bond between adjacent segments increases the stiffness at both segments, except if the unsaturation involves terminal chain segments. Using six-segment solutes as an example (for which calculated potencies are reported below) unsaturated chains with localized stiffness distribution $\{s, f, f, f\}$, would serve as a crude model of 1-hexyne or 1-hexene, whereas $\{s, s, f, f\}$ and $\{f, s, s, f\}$ would serve as models for 2-hexyne (or *trans*-2-hexene) and 3-hexyne (or *trans*-3-hexene), respectively. The multiply unsaturated hexanes 1,3-hexadiyne, 2,4-hexadiyne, 1,4-hexadiyne, and 1,5-hexadiyne (or more approximately, for the corresponding *trans*-dienes) would be represented as $\{s, s, s, f\}$, $\{s, s, s, s\}$, $\{s, f, s, s\}$, and $\{s, f, f, s\}$, respectively, and 1,3,5-hexatriyne would be $\{s, s, s, s\}$. Of course, the conformational flexibility f at an internal methylene group in, for example, 1,4-hexadiene or 1,4-hexadiyne is not identical to a methylene group in hexane, but for simplicity, only one value of the stiffness, $\omega_{flex} = 0.45$, is used to describe a saturated carbon in the calculations, regardless of its neighbors. Unfortunately, a precise specification of the value of ω_{rod} is difficult, so in the present work results are reported for calculations using $\omega_{rod} = 0.15$ (threefold lower probability of a chain bend compared to saturated alkane chains, as used for perfluorination) as a likely representative value for both alkynes and *trans*-alkenes.

Solute: interfacial activity of chain segments

Each segment of the solute can be characterized by an interfacial exchange energy ϵ, i.e., the energy to exchange it from the membrane interior with a segment of the lipid "solvent" (a CH_2 group) at the aqueous interface. Clearly, the interfacial attraction of a hydroxyl group is very strong ($\epsilon < 0$, with $|\epsilon| \gg k_BT$), arising largely from its ability to donate a hydrogen bond, whereas the exchange energy of a solute CH_2 group is zero by definition. There are smaller differences among CH_2, CF_2, CH_3, and CF_3 groups as well. Results of molecular dynamics simulations (Cui et al., 1998) suggest a net interfacial attraction of CH_3 groups, a much smaller attraction of CF_3 groups, but a positive interfacial exchange energy (effectively an interfacial repulsion) for CF_2. For simplicity, and because getting accurate numerical estimates of the strength of these interactions is difficult, these differences in interfacial interactions are ignored in the present work, as are the differences in exchange pairwise interaction energies among CH_2, CF_2, CH_3, and CF_3 groups. However, they may well underlie the marked differences in membrane distribution (North and Cafiso, 1997) and anesthetic potencies (Koblin et al., 1994) among cyclobutanes of different degrees of fluorination.

In addition to causing increased stiffness, the presence of unsaturation in hydrocarbon chains is likely to result in a greater attraction to the aqueous interface (as compared to saturated bonds between adjacent methylene groups), characterized by an interfacial attraction per unsaturated segment $\epsilon_u < 0$. This net attraction is presumably larger for segments involved in triple bonds than in double bonds, and would be expected to increase in magnitude for molecules with delocalized pi-orbitals, such as conjugated polyenes. It is difficult to quantify this interfacial attraction, so

calculations have been performed for a range of plausible values ($-k_BT \leq \epsilon_u < 0$).

Lipid characteristics

The properties of the bilayer depend not only on the characteristics of the solutes but of the lipid solvent as well. Variation in head group repulsions, acyl chain unsaturation, and incorporation of cholesterol are all predicted (Cantor, 1999a) to have a significant effect on the pressure distribution and on the perturbation of that distribution by solutes. For simplicity, in the present work, only saturated 16-carbon (palmitoyl) acyl chains are considered, described by a uniform chain stiffness $\omega[(CH_2)_x] \approx 0.45$. However, effects of varying head group repulsion are considered. It has been shown (Stigter et al., 1992) that the electrostatic interactions among phosphatidylethanolamine (PE) head groups are small and relatively insensitive to changes in temperature, whereas the repulsions among phosphatidylcholine (PC) head groups are strong and increase significantly with rising temperature. In the context of a simple mean-field approach (Cantor, 1999a), head group interactions can be modeled as a pairwise additive energy that varies inversely with molecular area, with constant of proportionality u_{hg} that is a measure of the strength of the average repulsion of adjacent head groups. For pure PC, u_{hg}(PC) is roughly 1 to 1.5 in units of k_BT (the value depending on temperature), and u_{hg}(PE) ≈ 0. Note that for a mixture of head groups, the effective u_{hg} is the average of all pairwise interactions; thus a 50/50 mix of PC and PE would have $u_{hg} \approx 1/4\ u_{hg}$(PC). Although it is difficult to estimate the value precisely, the lipid head group composition of a representative synaptic membrane might be expected to have u_{hg} of order 0.3 to $0.5k_BT$; we present results of calculations for $u_{hg} = 0$, 0.4, and 0.8 k_BT to span the range of likely values.

RESULTS

Intrinsic potencies

Alkanes and monohydric alkanols

Fig. 1 *a* displays predictions of intrinsic potency S as a function of chain length for semiflexible solutes ($\omega = 0.45$) with no interfacial attraction of any segment ($\epsilon_1 = \epsilon_2 = \cdots = \epsilon_n = 0$), as a model of alkanes, and with a large interfacial attraction of the first segment only ($\epsilon_1 = -10k_BT$, characteristic of a typical hydrogen bond strength, with $\epsilon_2 = \epsilon_3 = \cdots = \epsilon_n = 0$), as a model for strongly amphiphilic solutes such as 1-alkanols. These results are obtained using a range of values of the lipid head group pair repulsion energy u_{hg}, as discussed above. Clearly, for short chains, the attraction of one end of the molecule to the aqueous interface results in a much greater potency, i.e., a much greater net shift in the pressure profile away from the center of the bilayer. However, with increasing chain length of the amphiphilic solutes, a marked decrease in intrinsic potency is predicted, eventually approaching zero (cutoff). The magnitude of the average lipid head group repulsion is important; at intermediate values, a cutoff is predicted at about 12 to 14 carbons. For solutes without any interfacial attraction, the intrinsic potency is fairly low for short chains, and in the presence of lipid head group repulsions, decreases through zero, with a cutoff at smaller n than for amphiphilic solutes.

The effect of increasing solute stiffness uniformly along the entire molecule (reducing ω from 0.45 to 0.15) is shown in Fig. 1 *b*. Unlike the results shown in Fig. 1 *a*, the decrease in intrinsic potency is extremely rapid for the amphiphilic solutes, regardless of lipid head group repulsion, with a much shorter cutoff predicted at $n \sim 4$ or 5. For longer stiff amphiphiles, the potency is calculated to be large in magnitude but of opposite sign, i.e., a large negative anesthetic effect is predicted. For chains without interfacial activity, the increase in stiffness has a somewhat milder effect on the shape of the curve, but since S is small even for short chains, the cutoff is predicted to drop to only 3 or 4 segments.

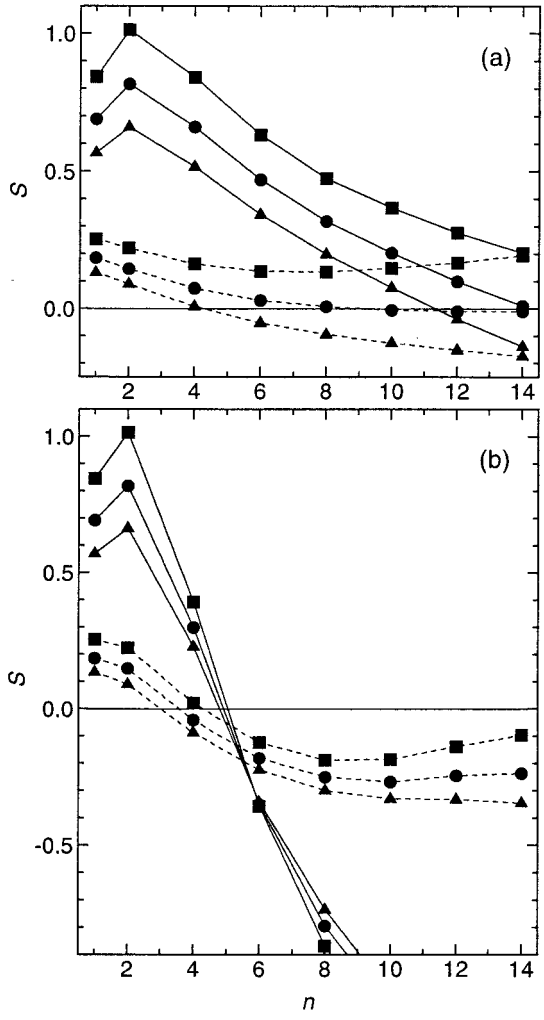

FIGURE 1 Intrinsic potency, S, as a function of solute chain length, n, for solutes of the form $\mathbf{C}_n$, i.e., with no interfacial attraction (*dotted lines*) and for solutes of the form $\mathbf{AC}_{n-1}$, i.e., with strong interfacial attraction for the first segment only (*solid lines*). Lines are drawn only as a guide to the eye. (*a*) Semiflexible chains ($\omega = 0.45$). (*b*) Chains with greater (linear) stiffness ($\omega = 0.15$). Lipid head group repulsion: $u_{hg}/k_BT = 0.0$ (■), 0.4 (●), 0.8 (▲). For ease of comparison, the two panels are plotted using the same ordinate scale.

If the predictions portrayed in Fig. 1, *a* and *b*, are accurate, then only the long-chain, stiff amphiphilic molecules, (large n for solid lines in Fig. 1 *b*) are predicted to have large negative intrinsic potencies. These might correspond best to

long-chain perfluorinated alkanols; for the choice of parameters used ($\omega = 0.15$, and no interfacial activity for any but the first segment) the effect is not predicted to be of large magnitude until n $\approx$ 8. The most closely related experimental work is that of Eger et al. (1999a) on 1-alkanols that are perfluorinated on all but the hydroxylated carbon (and thus somewhat less stiff). They find a clear trend with increasing chain length n from strong intrinsic potency at $n = 2$ to nonanesthetic at $n \approx 7$ or 8, qualitatively consistent with the predictions, although the crossover occurs at somewhat higher chain length than predicted, which may result from the fact that the first carbon is hydrogenated. However, additivity studies were not performed for longer chain lengths, which according to the predictions of the present work would be required for negative intrinsic potency to be observed. It has recently been shown (Ueno et al., 1999) that unlike the shorter-chain analogues, $CF_3(CF_2)_5CH_2OH$ decreases the potentiation of $GABA_A$ (γ-aminobutyric acid) receptor response to isoflurane (and pentobarbital) expressed in *Xenopus* oocytes.

Additivity studies have also been performed (Liu et al., 1994a) for perfluoroalkanes. The predictions (dashed lines in Fig. 1 *b*) indicate that stiff, interfacially inactive molecules show only a mildly negative potency, and then only for $n \geq 6$ or so. The studies of Liu et al. (1994a) are inconclusive in that C_4F_{10} and C_5F_{12} do show mild negative potency, i.e., a 30% increase in MAC of halothane and isoflurane (but not desflurane), whereas C_6F_{14} shows no negative potency in additivity studies with isoflurane or halothane. Liu et al. (1994a) found that only CF_4 had anesthetic potency (using MAC as the anesthetic endpoint), whereas in earlier studies (Miller et al., 1972) using abolition of the righting reflex in mice as the endpoint, it was found that CF_4, C_2F_6, and C_3F_8 were anesthetics (the C_3F_8 results were obtained from additivity studies with N_2O.)

The results on alkanols described above only consider the interfacially active (hydroxyl) group on the terminal methyl segment, corresponding to 1-alkanols. Calculations have also been performed to predict the effect of varying the position, labeled j, of the single interfacially active segment (i.e., the hydroxymethylene group) along the alkanol chain. (For alkanols, for simplicity of notation, chain segments with $\epsilon \approx 0$, corresponding to -CH_2- or -CH_3 groups are labeled **C**, and those with strong interfacial attraction, such as -CHOH- or -CH_2OH, are labeled **A**. Thus, alkanes of length n are symbolized as $\mathbf{C}_n$, 1-alkanols as $\mathbf{AC}_{n-1}$, 2-alkanols as $\mathbf{CAC}_{n-2}$, α,ω-diols as $\mathbf{AC}_{n-2}\mathbf{A}$, etc.). Fig. 2 shows results for alkanols of two representative chain lengths, $n = 9$ and $n = 13$, with the hydroxyl at position $j = 1, 2, \ldots, (n + 1)/2$, i.e., from the terminal methyl group ($\mathbf{AC}_{n-1}$) to the central methylene group ($\mathbf{C}_{(n-1)/2}\mathbf{AC}_{(n-1)/2}$). For a given n, the intrinsic potency is predicted to be lowest by far for the 1-alkanols, i.e., for $j = 1$; moving the hydroxyl toward the middle of the chain is predicted to result in a sharp increase in potency up to roughly the third segment,

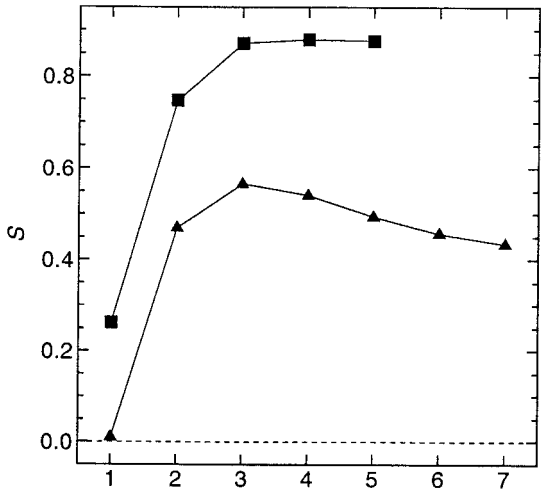

FIGURE 2 Intrinsic potency, S, of semiflexible solutes of the form $\mathbf{C}_{j-1}\mathbf{AC}_{n-j}$, i.e., with a single segment with strong interfacial attraction **A** as a function of the position j of that segment along the chain. This serves as a model of monohydric alkanols of fixed length but of varied position of the hydroxyl group along the chain. Results are presented for two chain lengths: $n = 9$ (■) and $n = 13$ (▲). All calculations were performed with head group repulsion $u_{hg}/k_BT = 0.4$. Lines are drawn only as a guide to the eye.

beyond which the potency varies relatively little as the hydroxyl is moved toward the center of the chain. This marked increase in potency is to be expected, since a flexible chain strongly attracted to the aqueous interface at or near its center should behave similarly to two 1-alkanol molecules of roughly half the chain length. Because shorter alkanols have greater intrinsic potency (Fig. 1), and because there are effectively twice as many molecules, the increase in potency is large. Although octanol/water and bilayer/water partition coefficients have been reported for octanols with hydroxyl group at different positions on the chain (Hansch and Dunn, 1972; Jain and Wray, 1978), no experimental information is available on their anesthetic potencies, so a comparison to predicted intrinsic potencies is not yet possible.

Polyhydric alkanols

Predictions have also been obtained for longer hydrocarbon chains with multiple hydroxyl groups. One group of calculations involves chains with interfacially active segments spaced at regular intervals (every L segments) along the chain between the first and last segments; using the notation described above, these alkanols can be represented as $(\mathbf{AC}_{2M})_y\mathbf{A}$, with $2M = L - 1$, and $y = (n - 1)/L = 1, 2, 3, \ldots$. Such molecules, which are regularly tethered to the interface, might be expected to behave like $2y$ short 1-alkanol chains, each of effective length $n^* = M + 1$. As an example, $(\mathbf{AC}_4)_3\mathbf{A}$, which corresponds most closely to

1,6,11,16-hexadecanetetraol, has values of $2y = 6$ and $n^* = 3$, and thus might be expected to have potency $S[(\mathbf{AC}_4)_3\mathbf{A}] \approx 6\, S(\mathbf{AC}_2)$, where $\mathbf{AC}_2$ corresponds most closely to 1-propanol. Using similar reasoning, the results for alkanols with one hydroxyl group at the center of the chain can be generalized to oligomers of the form $(\mathbf{C}_M\mathbf{AC}_M)_y$, where $y = n/L = 1, 2, 3, \ldots$, again defining $2M = L - 1$. Such solutes might analogously be expected to behave similarly to $2y$ short 1-alkanol chains, each of effective length $n^* = M + 1$. As an example, $(\mathbf{C}_3\mathbf{AC}_3)_2$, which corresponds most closely to 4,11-tetradecanediol, has values of $2y = 4$ and $n^* = 4$, and thus might be expected to exhibit an intrinsic potency $S[(\mathbf{C}_3\mathbf{AC}_3)_2] \approx 4\, S(\mathbf{AC}_3)$, where $\mathbf{AC}_3$ corresponds most closely to 1-butanol.

Results for a wide range of such polyhydric alkanols are presented in Fig. 3 *a*, in which the potencies S are plotted as a function of chain length n. Clearly, the potencies are predicted to get very large compared to even the largest values for short alkanols. Within a given series of either type, $(\mathbf{C}_M\mathbf{AC}_M)_y$ or $(\mathbf{AC}_{2M})_y\mathbf{A}$, the value of S increases nearly linearly with the oligomeric repeat index y, consistent with the above discussion. For given value of y, the intrinsic potency drops slowly with increasing M, i.e., with increasing separation between interfacially active segments. All of these results, i.e., for $(\mathbf{C}_M\mathbf{AC}_M)_y$ and for $(\mathbf{AC}_{2M})_y$A with $y \geq 1$ and thus for $2y > 1$, can be compared by replotting them in terms of the intrinsic potency per amphiphilic subgroup (equivalent short 1-alkanol) i.e., plotting $S^* = S/(2y)$ as a function of n^*, as shown in Fig. 3 *b*. The similarity of these reduced potencies is evident: all the predictions from Fig. 3 *a* fall roughly on a single curve in Fig. 3 *b*, similar to (but offset somewhat from) that for simple 1-alkanols, which is included for purposes of comparison. Unfortunately, there is little experimental data on potency of polyhydric alkanols to which these predictions can be compared. Moss et al. (1991) measured the potencies of α,ω-alkanediols; they observed no cutoff, but studied only diols of lengths up to $n = 12$. Extrapolation of the calculated results for α,ω-alkanediols to $S = 0$ predicts a cutoff in potency at $n > 20$; it would be interesting to see if this obtains experimentally. Unfortunately, partition coefficients have not been reported for the diols for which Moss et al. obtained aqueous EC_{50} values, so the prediction of an approximate doubling of their intrinsic potency can not presently be tested.

A nearly linear increase in intrinsic potency for oligomeric alkanols with increasing number of repeat units is predicted for all the oligomeric series for which calculations were performed. In principle, one can imagine that the hydrophobic/hydrophilic balance can be manipulated by varying the number of alkyl segments per hydroxyl group, which will presumably allow for tuning of the oil/water partition coefficient to an experimentally useful range. In a first approximation, increasing polymer index in such a series of molecules would be predicted to maintain an

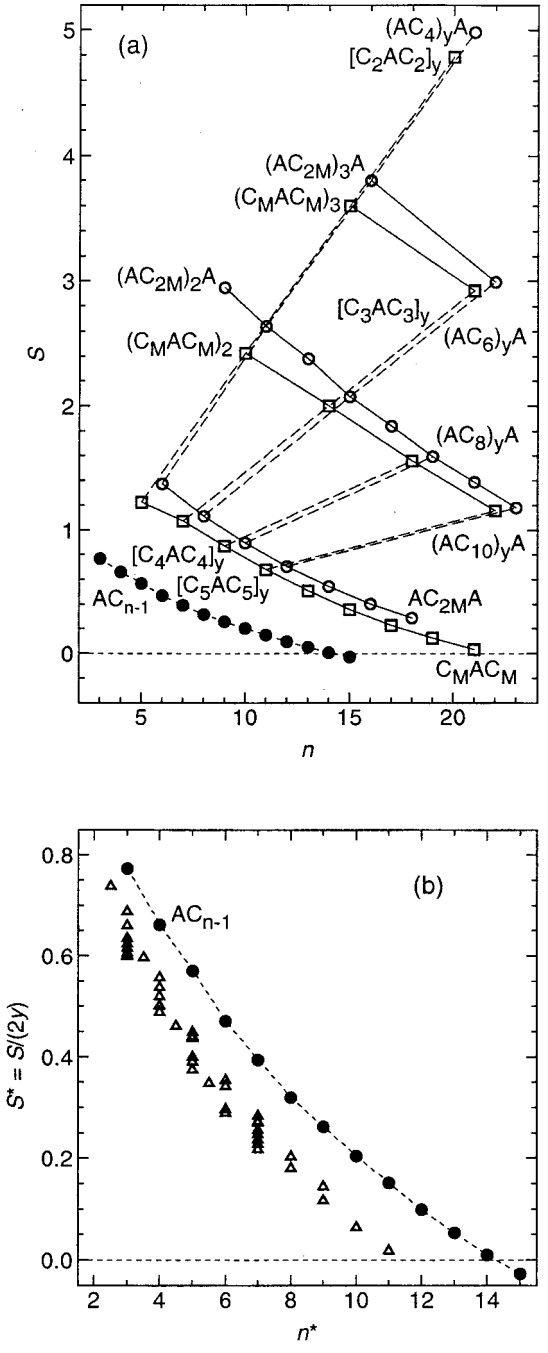

FIGURE 3 (*a*) Intrinsic potency, S, as a function of solute chain length, n, for alkanols of the general form $[\mathbf{C}_M\mathbf{AC}_M]_y$ (□) and of the form $[\mathbf{AC}_{2M}]_y\mathbf{A}$ (○), where **A** corresponds to a strongly interfacially active segment ($\epsilon \ll -k_BT$, as a model for -CH_2OH or -CHOH- groups) and **C** to an interfacially inactive segment ($\epsilon = 0$, as a model for -CH_3 or -CH_2- groups). The lines are drawn to group together solutes of a particular type and particular values of either M or y: *solid lines* for fixed y and varying M, and *dashed lines* for fixed M and varying y. (*b*) All results from (*a*) re-expressed (△) as a reduced intrinsic potency $S^* = S/(2y)$, i.e., the intrinsic potency per amphiphilic subgroup, as a function of the number of segments per subgroup $n^* = M + 1$. In both panels, results for solutes of the form $\mathbf{AC}_{n-1}$ (models of 1-alkanols) are provided (●, *dotted line*). Lipid head group repulsion $u_{hg}/k_BT = 0.4$ in all cases.

oil/water partition coefficient that is approximately constant, while increasing intrinsic potency roughly linearly, and thus increasing apparent potency approximately linearly, with no limit with respect to chain length, i.e., no cutoff.

Localized stiffness: unsaturated alkanes

It is interesting to examine the effect of increasing chain stiffness nonuniformly along the solute chain, as can be achieved by localized chain unsaturation or atomic substitutions. Molecules that differ with respect to local rigidity (and if rigid, whether rod-like or bent) but with otherwise identical characteristics (distribution of segmental interfacial activity) are predicted to have significantly different effects on the pressure distribution, as shown in Fig. 4 for the example of five-segment chains with no segmental interfacial activity. For an otherwise semiflexible (ω_{flex} = 0.45) chain, an increase in linear rigidity (ω_{rod} = 0.15) at any one of the segments is predicted to cause a reduction in intrinsic potency, the effect increasing roughly additively with the number of sites of increased linear stiffness. By contrast, a chain with a single rigid bend ($\omega_{bent} \gg 1$) is predicted to have significantly increased potency, although additional stiff bends in the molecule yield smaller increments in potency.

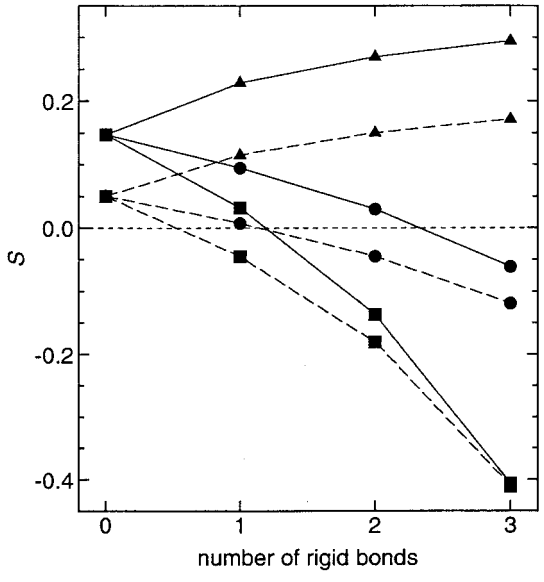

FIGURE 4 Intrinsic potency, S, of five-segment solutes without interfacial attraction but with nonuniform internal stiffness. The three internal segments are progressively replaced by stiffer bonds; either rod-like (●, ω = 0.15; ■, ω = 0.0) or rigidly bent (▲, $\omega \gg 1$). Results for both one and two rigid bonds represent, in each case, averages over the different possible spatial arrangements of the rigid bonds. Results are presented for two values of the head group repulsion: u_{hg}/k_BT = 0.0 (*solid lines*) and u_{hg}/k_BT = 0.4 (*dashed lines*). Lines are drawn only as a guide to the eye.

For hexynes or *trans*-alkenes, the local stiffness and increased interfacial activity (as compared to saturated alkanes) would be expected to have opposing effects on intrinsic potency. In Fig. 5 *a*, predictions of intrinsic potency for six-segment solutes of varying location and degree of unsaturation are plotted as a function of ϵ_u, the interfacial attraction of segments participating in unsaturated bonds. For purposes of comparison, the predicted potency for hexane $\{f,f,f,f\}$ is included. In Fig. 5 *b*, the results of Fig. 5 *a* are replotted as a function of $\epsilon_{mol} = 2n_u\epsilon_u$, the interfacial attraction per molecule. With regard to intrinsic potency, an increase in segmental interfacial activity can clearly compensate for increased linear stiffness, to a degree that, for given total stiffness, depends largely on the total molecular interfacial activity. However, regardless of the value of ϵ_u, a greater intrinsic potency is predicted for 1-hexyne, which is stiff only at one internal segment, than for 2- or 3-hexyne, which have approximately the same interfacial attraction as 1-hexyne, but two sites of chain stiffness.

Segment distributions

At present, there is no experimental method by which the lateral pressure profile can be measured. So it would be valuable to find other, more readily measurable properties, the changes in which are at least qualitatively related to changes in the pressure distribution. The depth-dependent probability distribution of solute segments $\psi(z)$, i.e., the likelihood of finding a segment of the solute at a given membrane depth, independent of the location of the segment along the solute chain, might be expected to serve as such a property since it can, in principle, be measured, and is obtained from the statistical mechanical approach used to calculate the lateral pressure profiles. For small, strongly interfacially active solutes, such as short 1-alkanols, the predicted large increase in pressures near the aqueous interface is certainly related to the fact that the segments of the solute are localized in the region where the pressures increase, and this is consistent with the difference in spatial distributions of some anesthetics and nonimmobilizers (North and Cafiso, 1997; Tang et al., 1997; Chipot et al., 1997). However, this correlation does not hold in a comparison of molecules of similar interfacial activity, but of different stiffness, as shown by comparison of the results in Figs. 1 and 6. In Fig. 6 *a*, plots of $\psi(z)$ are reported over a range of chain lengths, for solutes $\mathbf{C}_n$, i.e., with no interfacial activity (ϵ_i = 0, i = 1, . . . , n) and of the same flexibility as the lipid acyl chains (ω = 0.45). For very short chain solutes, which are predicted to have small positive intrinsic potencies, the segment probability distribution is nearly uniform, but with increasing chain length, the distribution becomes strongly skewed toward the center of the bilayer, consistent with neutron diffraction experiments of White et al. (1981) on hexane. Comparison of these results with the chain length dependence of the intrinsic potency,

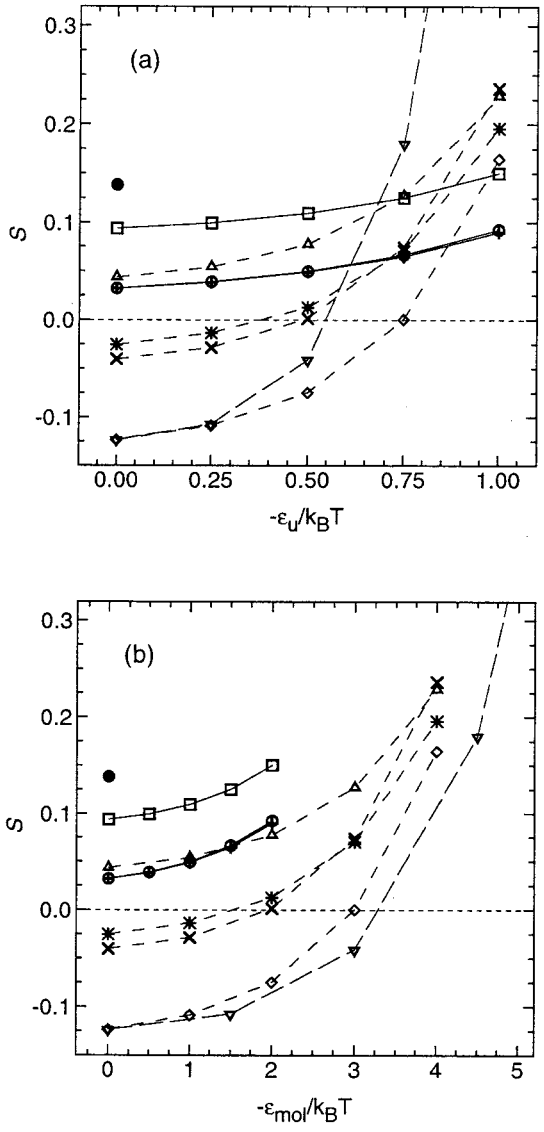

FIGURE 5 Effect of interfacial activity of unsaturated segments on the calculated intrinsic potency, S, of six-segment solutes (as models of hexynes or *trans*-hexenes). (*a*) S is plotted as a function of $-\epsilon_u$, the magnitude of the interfacial attractive energy per unsaturated segment, in units of k_BT. (*b*) Same data as in (*a*), but plotted as a function of the magnitude of the interfacial attractive energy per molecule, $-\epsilon_{mol} = -2n_u\epsilon_u$ (in units of k_BT) where n_u is the number of unsaturated bonds (and thus $2n_u$ is the number of unsaturated segments) in the molecule. $n_u = 1$ (*solid lines*): 1-hexyne $\{s, f, f, f\}$, (□); 2-hexyne $\{s, s, f, f\}$, (○); 3-hexyne $\{f, s, s, f\}$, (+). $n_u = 2$ (*short dashed lines*): 1,3-hexadiyne $\{s, s, s, f\}$, (×); 1,4-hexadiyne $\{s, f, s, s\}$, (*); 1,5-hexadiyne $\{s, f, f, s\}$, (△); 2,4-hexadiyne $\{s, s, s, s\}$, (◇); $n_u = 3$ (*long dashed line*): 1,3,5-hexatriyne $\{s, s, s, s\}$, (▽). Predictions for the fully saturated hexane $\{f, f, f, f\}$, (●), are included for purposes of comparison. In the above list, the flexibility of the four interior bonds are indicated by *s* (stiff, $\omega = 0.15$) or *f* (semiflexible, $\omega = 0.45$). For all calculations, $u_{hg}/k_BT = 0.0$.

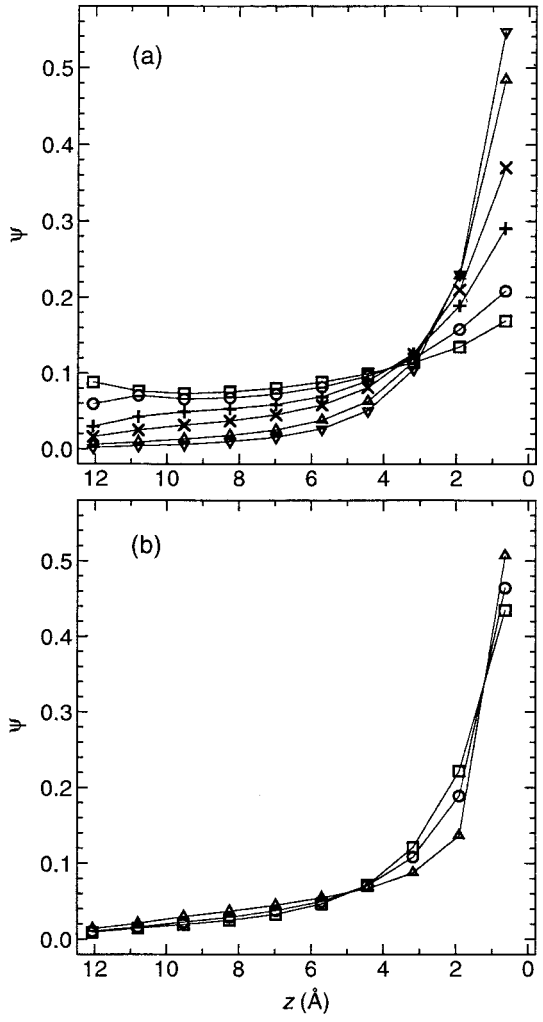

FIGURE 6 Spatial probability distribution $\psi(z)$ of segments of solutes with no interfacial activity ($\epsilon_i = 0$, $i = 1, \ldots, n$) for varying chain length (n) and stiffness (ω). Bilayer depth z(Å) indicates the distance from the bilayer midplane (in either direction, since the bilayer is symmetric). (*a*) Semiflexible chains ($\omega = 0.45$) of length $n = 1$ (□), 2 (○), 4 (+), 6 (×), 10 (△), and 14 (▽). (*b*) Fixed alkane chain length $n = 8$, for varying chain stiffness: $\omega = 0.45$ (□), 0.30 (○), and 0.15 (△).

one might conclude that potency is lost when the segment distribution shifts strongly toward the membrane interior. However, different conclusions are reached when the stiffness of the solute is increased at fixed chain length. In Fig. 6 *b*, the spatial distribution is plotted as a function of increasing chain stiffness, for $n = 8$ segment solutes. The increase in stiffness is predicted to have a small effect on the probability distribution, if any, causing a shift from the interior toward the aqueous interface. However, the increased stiffness is predicted to cause a loss in intrinsic potency, as seen in a comparison of Fig. 1, *a* and *b*. Results for alkanes of other chain lengths are similar.

In Fig. 7 *a*, the segment probability distribution $\psi(z)$ is plotted for a range of chain lengths for 1-alkanols ($\mathbf{AC}_{n-1}$), i.e., for semiflexible solutes ($\omega = 0.45$) with one end attracted to the interface ($\epsilon_1 = -10$, $\epsilon_i = 0$, $i = 2, \ldots, n$). Increasing the chain length of semiflexible 1-alkanols is

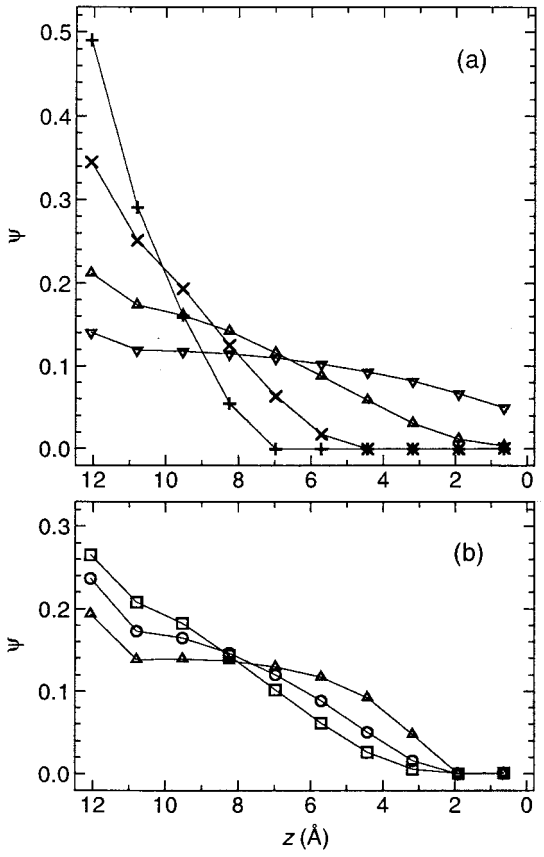

FIGURE 7 Spatial probability distribution $\psi(z)$ of segments of 1-alkanols ($\epsilon_1 = -10\ k_BT$; $\epsilon_i = 0$, $i = 2, \ldots, n$) for varying chain length (n) and stiffness (ω). Bilayer depth z(Å) indicates the distance from the bilayer midplane. (*a*) Alkanols (semiflexible chains, $\omega = 0.45$) of length $n = 4$ (+), 6 (×), 10 (△), and 14 (▽). (*b*) Fixed 1-alkanol chain length $n = 8$, for varying chain stiffness: $\omega = 0.45$ (□), 0.30 (○), and 0.15 (△).

predicted to cause a marked shift of the segment distribution toward the bilayer interior, and is accompanied by a more gradual decrease in intrinsic potency (Fig. 1 *a*). In Fig. 7 *b*, plots of $\psi(z)$ are presented over a range of chain stiffnesses for alkanols of length $n = 8$. The increase in stiffness at fixed chain length is predicted to result in a less pronounced shift in the segment distribution than seen in Fig. 7 *a* for an increase in length at fixed stiffness, but is accompanied by a much greater drop in potency (to very negative values). Unfortunately, from the results presented in Figs. 6 and 7, it seems that there is no simple predictive relation between the intrinsic potency of a solute and the depth distribution of its segments.

Apparent potencies

The approach described above predicts the chain length dependence of the intrinsic potency for linear molecules of varying interfacial activity and stiffness. Although the intrinsic potency is a more fundamental measure of potency in the framework of an indirect mechanism of anesthesia, apparent potencies are much more commonly used to express experimental results, so it may be useful to re-express the predictions in terms of apparent potencies to facilitate comparison with experiment.

The Meyer-Overton correlation, extended to account for differences in intrinsic potency, can be expressed as $S\,c_o^* =$ constant, where the oil (bilayer) concentration is given by

$$c_o^* = K_{o/w}c_w^* = K_{o/g}c_g^*$$

and thus

$$c_g^* \propto (SK_{o/g})^{-1} \tag{2}$$

for inhalation anesthetics, with a single constant of proportionality (for given bilayer composition). From Eq. 2, the change in c_g^*, and thus the change in the apparent potency, can be determined within a homologous series of compounds that differ only in chain length. For solutes such as alkanes and many alkane derivatives, $K_{o/g}$ varies roughly exponentially with chain length; since $n - 2$ represents the number of interior segments, then

$$K_{o/g} \approx K_0\lambda_{o/g}^{n-2} \tag{3}$$

where K_0 is the partition coefficient for solutes with $n - 2 = 0$ interior segments, and $\lambda_{o/g} > 1$ is the multiplicative increase in $K_{o/g}$ per added interior segment. As a rough guide, $\lambda_{o/g} \approx 3$ for CH_2 segments, while for CF_2 segments $\lambda_{o/g} \approx 2$ (Eger et al., 1999a). Within a homologous series, the gas-phase concentration of an anesthetic with $n - 2$ interior segments, c_g^*, relative to that of a solute with no interior segments, $c_g^*(0)$, is obtained from Eqs. 2 and 3:

$$\log_{10}[c_g^*/c_g^*(0)] \approx -(n-2)\log_{10}\lambda_{o/g} - \log_{10}(S/S_0) \tag{4}$$

The analysis leading to Eq. 4 can also be expressed in terms of aqueous potencies as

$$\log_{10}[c_w^*/c_w^*(0)] \approx -(n-2)\log_{10}\lambda_{o/w} - \log_{10}(S/S_0) \tag{5}$$

although for CH_2 groups, $\lambda_{o/w}$ is somewhat larger than $\lambda_{o/g}$; of order 3.5 to 4.0. Predictions using Eq. 4 for the dependence of apparent potency on chain length are plotted in Fig. 8 for the same solutes for which calculations of intrinsic potencies are presented in Fig. 1. Clearly, for alkanes, alkanols, and perfluorinated alkanols, an increase in apparent potency accompanies a decrease in intrinsic potency with increasing chain length. These predicted trends are qualitatively similar to the results summarized recently by Eger et al. (1999a,b).

DISCUSSION

The results presented here, based on statistical thermodynamic calculations using a mean-field lattice model to describe the conformational statistics of acyl chain packing,

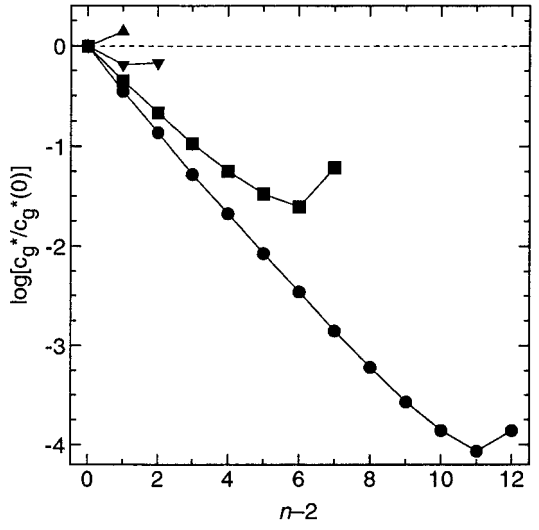

FIGURE 8 Predicted gas-phase apparent potency c_g^* of solutes of length n (with $n-2$ interior segments) relative to the predicted apparent potency $c_g^*(0)$ of a solute of the same type but of length $n = 2$ (i.e., with no interior segments) as a function of $(n-2)$, the number of interior segments. The data are calculated using the approximate relation of Eq. 4, i.e., as $\log[c_g^*/c_g^*(0)]$, using intrinsic potencies calculated for $u_{hg}/k_BT = 0.4$. Results are presented for models of 1-alkanols [$\omega = 0.45$; $\epsilon_1 = -10k_BT$; $\epsilon_i = 0$, $i = 2, \ldots, n$; $\lambda_{o/g} = 3.0$, (●)], perfluorinated alkanols [$\omega = 0.15$; $\epsilon_1 = -10k_BT$; $\epsilon_i = 0$, $i = 2, \ldots, n$; $\lambda_{o/g} = 2.0$, (▼)], alkanes [$\omega = 0.45$; $\epsilon_i = 0$, $i = 1, \ldots, n$; $\lambda_{o/g} = 3.0$, (■)], and perfluorinated alkanes [$\omega = 0.15$; $\epsilon_i = 0$, $i = 1, \ldots, n$; $\lambda_{o/g} = 2.0$, (▲)].

demonstrate that the influence of hydrophobic or amphiphilic solutes on the bilayer pressure profile depends sensitively on chain length and particularly on the distribution of interfacial activity and stiffness over the length of the solute chain. The large differences in intrinsic potencies among alkanes, alkanols, and their fluorinated counterparts, including the well-known cutoffs in anesthetic potency with increasing chain length, correlate remarkably well with the predictions of intrinsic potency based on the influence of the resulting changes in the pressure distribution on protein conformational equilibria. In particular, the differences in cutoffs for different types of solute chains are qualitatively correctly predicted.

Intrinsic potencies are predicted for a range of monohydric and polyhydric alkanols for which potencies have not yet been measured, but which would serve as an excellent test of the pressure profile mechanism. Predicted intrinsic potencies for monohydric alkanols in which the hydroxyl group is placed on an interior chain segment are predicted to be much greater than for 1-alkanols of the same length. Alkanols of length n with a single hydroxyl group near the middle of the chain are predicted have roughly twice the potency of 1-alkanols of chain length $\approx n/2$; consequently, the cutoff for such alkanols is predicted to occur at a length $n > 20$. In general, chains that are regularly tethered to the aqueous interface, such as polyhydric alkanols with hydroxyl groups regularly spaced along the chain, are predicted to act similarly to a collection of shorter 1-alkanol chains of length roughly equal to half the spacing between hydroxyl groups on the chain. The intrinsic potency of such polyhydric alkanols should thus increase with the number of repeat units, without limit; certainly no cutoff would be expected. A measurement of the potencies of such molecules would thus distinguish between indirect and direct binding mechanisms of anesthesia, since no binding site could possibly accommodate a molecule without limit in size, the potency of which only increases with size. Although this argument is made in the context of polyhydric alkanols, it would be expected to hold for other oligomers with regularly spaced interfacially active segments, such as polyethers and polyacids, or if the hydroxyl group is attached to the alkane backbone through a short alkyl spacer.

The predicted sensitivity of pressure redistribution to increased solute stiffness implies that rod-like, interfacially inactive molecules should be nonimmobilizers, whether or not the stiffness is due to perfluorination. However, other molecular manipulations that cause increased chain linear rigidity, such as the incorporation of chain unsaturation, will likely be accompanied by increased interfacial activity, which has the opposite effect on the pressure distribution. Unfortunately, an approximate measure of the strength of the interfacial activity (such as approximate Lennard-Jones parameters for united-atom carbons involved in multiple bonds) is not presently available, so a simple comparison of the intrinsic potencies of alkanes and alkynes, for example, will not yet serve as a test of this mechanism. Still, molecules having the same total unsaturation (and thus the same interfacial attraction) but with different degrees of internal stiffness are clearly predicted to have different potency. For example, chain molecules with unsaturation located at the terminal methyl groups are more flexible, and thus should have higher intrinsic potency, than those with the same degree of unsaturation located at interior bonds. Thus, 1-hexyne is predicted to have higher intrinsic potency than 2- or 3-hexyne.

On the plausibility of indirect (bilayer-mediated) mechanisms of anesthesia

It has been suggested by various authors (Franks and Lieb, 1994; Krasowski and Harrison, 1999) that in light of much of the research on anesthetic mechanisms over the past few decades, it is very unlikely that anesthesia proceeds by any indirect, lipid-mediated mechanism. Three classes of arguments are presented. The first concern is the anomalous lack of potency of some membrane-soluble molecules, i.e., the significant deviations from the Meyer-Overton correlation. The results presented here demonstrate that the anomalously low potency of some membrane-soluble compounds not only can be rationalized, but is in fact predicted (as is the anomalously high potency of other compounds) in the con-

text of an indirect mechanism based on the lateral pressure distribution.

A second argument involves the magnitude of the effects of anesthetics on bilayer properties at clinically relevant concentrations of anesthetics. It is often noted that the more readily measured bilayer properties (thickness, fluidity, etc.) are only slightly altered by incorporation of anesthetics, and that the changes in these properties can be reproduced by a slight increase in temperature, which certainly does not cause anesthesia; on the contrary, a decrease in body temperature can mimic anesthetic effects. The redistribution of lateral pressures is a remarkable counter-example, in terms of both the likely magnitude of the effect on protein equilibria and the effect of temperature. As discussed in detail elsewhere (Cantor, 1999a,b), the presence of two lipid/water interfaces, each of which results in a large interfacial tension, requires balancing (positive) lateral forces in the membrane interior, which, being concentrated over a few nanometers, results in lateral pressure densities in the membrane interior that are of enormous magnitude (many hundreds of atmospheres). Thus, a relatively small redistribution of these extremely large stresses is predicted to be sufficient to induce a significant shift in protein conformational equilibria. The addition of a solute causes a depth-dependent redistribution of pressures, largely resulting from the nonuniform spatial and orientational distribution of the solute in the bilayer, whereas a change in temperature is likely to result in a small and relatively uniform shift in the pressure distribution. For example, a drop in temperature results in a decrease in the repulsions among phosphatidylcholine head groups (Stigter et al., 1992), causing a compensating increase in lateral pressures spread through the bilayer interior, but not a sharp redistribution within the interior. As mentioned in the Introduction, the increase in apparent potencies (when measured through gas-phase concentrations) with decreasing temperature of most inhalation anesthetics results largely from an increase in oil/gas partition coefficients (Franks and Lieb, 1982), leaving the clinically relevant membrane concentration relatively independent of temperature, consistent with the predictions based on the lateral pressure profile mechanism.

The third argument involves stereoselectivity, i.e., the differential potency demonstrated by enantiomeric pairs, such as the mild difference between the enantiomers of isoflurane, and much larger differences in some larger intravenous anesthetics. Given that the lipids that comprise the bilayer are enantiomerically pure, with a chiral center located in the glycerol moiety, it is likely that the local interactions between the anesthetic and the lipid will differ for the two enantiomers of the anesthetic; altered local packing could certainly result in differential effects on the stress distribution, particularly as many anesthetics partition nonuniformly in the bilayer, with a preference for the region in which the glycerol linkage between the acyl chains and head group of the lipids is concentrated. It is important to note that colligative properties of the bilayer based on solvent equilibria, such as freezing point depression, would not be expected to depend on the choice of solute enantiomer, even though the lipid "solvent" is enantiomerically pure. As in bulk systems, colligative properties such as osmotic pressure, Raoult's law, and freezing point depression depend only on the decrease in chemical potential of the solvent that accompanies addition of a solute impurity (that is soluble only in the fluid solvent phase), which, at low concentrations, results purely from an increase in translational entropy, independent of the identity of the solute. That the freezing point depression of the main phase transition in a pure lipid bilayer is identical at the same aqueous concentrations of the two isomers of isoflurane (Franks and Lieb, 1991) is evidence that the aqueous/bilayer partition coefficients of the two enantiomers are identical, but has no bearing on the plausibility of a lipid-mediated mechanism of general anesthesia.

REFERENCES

Ben-Shaul, A. 1995. Molecular theory of chain packing, elasticity and lipid-protein interaction in lipid bilayers. *In* Structure and Dynamics of Membranes. R. Lipowsky and E. Sackmann, eds. Elsevier/North Holland, Amsterdam. 359–401.

Ben-Shaul, A., and W. M. Gelbart. 1994. Statistical thermodynamics of amphiphile self-assembly: structure and phase transitions in micellar solutions. *In* Micelles, Membranes, Microemulsions, and Monolayers. W. M. Gelbart, A. Ben-Shaul, and D. Roux, eds. Springer-Verlag, New York. 1–104.

Brown, M. F. 1997. Influence of nonlamellar-forming lipids on rhodopsin. *Curr. Topics Membr.* 44:285–356.

Cantor, R. S. 1995. The stability of bicontinuous microemulsions: a molecular theory of the bending elastic properties of monolyaers comprised of ionic surfactants and nonionic cosurfactants. *J. Chem. Phys.* 103: 4765–4783.

Cantor, R. S. 1996. Theory of lipid monolayers comprised of mixtures of flexible and stiff amphiphiles in athermal solvents: fluid phase coexistence. *J. Chem. Phys.* 104:8082–8095.

Cantor, R. S. 1998. The lateral pressure profile in membranes: a physical mechanism of general anesthesia. *Tox. Lett.* 100:451–458.

Cantor, R. S. 1999a. Lipid composition and the lateral pressure profile in bilayers. *Biophys. J.* 76:2625–2639.

Cantor, R. S. 1999b. The influence of membrane lateral pressures on simple geometric models of protein conformational equilibria. *Chem. Phys. Lipids.* 101:45–56.

Cantor, R. S. 1999c. Solute modulation of conformational equilibria in intrinsic membrane proteins: Apparent "cooperativity" without binding. *Biophys. J.* 77:2643–2647.

Chipot, C., M. A. Wilson, and A. Pohorille. 1997. Interactions of anesthetics with the water-hexane interface: a molecular dynamics study. *J. Phys. Chem. B.* 101:782–791.

Cui, S. T., J. I. Siepmann, H. D. Cochran, and P. T. Cummings. 1998. Intermolecular potentials and vapor-liquid phase equilibria of perfluorinated alkanes. *Fluid Phase Equilib.* 146:51–61.

deKruijff, B. 1997. Lipid polymorphism and biomembrane function. *Curr. Opin. Chem. Biol.* 1:564–569.

Eckenhoff, R., and J. S. Johansson. 1997. Molecular interactions between inhaled anesthetics and proteins. *Pharm. Rev.* 49:343–367.

Eger, E. I., J. Liu, D. D. Koblin, M. J. Laster, S. Taheri, M. J. Halsey, P. Ionescu, B. Chortkoff, and T. Hudlicky. 1994. Molecular-properties of the ideal inhaled anesthetic: studies of fluorinated methanes, ethanes, propanes, and butanes. *Anesth. Analg.* 79:245–251.

Eger, E. I., P. Ionescu, M. J. Laster, D. Gong, T. Hudlicky, J. J. Kendig, R. A. Harris, J. R. Trudell, and A. Pohorille. 1999a. Minimum alveolar anesthetic concentration of fluorinated alkanols in rats: relevance to theories of narcosis. *Anesth. Analg.* 88:867–876.

Eger, E. I., M. J. Halsey, R. A. Harris, D. D. Koblin, A. Pohorille, J. C. Sewell, J. M. Sonner, and J. R. Trudell. 1999b. Hypothesis: volatile anesthetics produce immobility by acting on two sites approximately five carbon atoms apart. *Anesth. Analg.* 88:1395–1400.

Epand, R. M. 1996. The properties and biological roles of non-lamellar forming lipids. *Chem. Phys. Lipids.* 81 and 82:101–264.

Fang, Z., P. Ionescu, B. S. Chorthoff, L. Kandel, J. Sonner, M. J. Laster, and E. I. Eger. 1997. Anesthetic potencies of *n*-alkanols: results of additivity and solubility studies suggest a mechanism of actin similar to that for conventional inhaled anesthetics. *Anesth. Analg*. 84:1042–1048.

Franks, N. P., and W. R. Lieb. 1978. Where do general anesthetics act? *Nature.* 274:339–342.

Franks, N. P., and W. R. Lieb. 1982. Molecular mechanisms of general anesthesia. *Nature*. 300:487–493.

Franks, N. P., and W. R. Lieb. 1986. Partitioning of long-chain alcohols into lipid bilayers: implications for mechanisms of general anesthesia. *Proc. Natl. Acad. Sci. USA.* 83:5116–5120.

Franks, N. P., and W. R. Lieb. 1991. Stereospecific effects of inhalational general anesthetic optical isomers on nerve ion channels. *Science.* 254: 427–430.

Franks, N. P., and W. R. Lieb. 1994. Molecular and cellular mechanisms of general anaesthesia. *Nature.* 367:607–614.

Gruner, S. 1991. Lipid membrane curvature elasticity and protein function. *In* Biologically Inspired Physics. L. Peliti, ed. Plenum Press, New York. 127–135.

Hansch, C., and W. J. Dunn. 1972. Linear relationships between lipophilic character and biological activity of drugs. *J. Pharm. Sci.* 61:1–19.

Harris, D., and A. Ben-Shaul. 1997. Conformational chain statistics in a model lipid bilayer: comparison between mean-field and Monte Carlo calculations. *J. Chem. Phys.* 106:1609–1619.

Hui, S. W. 1997. Curvature stress and biomembrane function. *Curr. Topics Membr.* 44:541–563.

Israelachvili, J., S. Marcelja, and R. Horn. 1980. Physical principles of membrane organization. *Q. Rev. Biophys.* 13:121–200.

Jain, M. K., and L. V. Wray, Jr. 1978. Partition coefficients of alkanols in lipid bilayer/water. *Biochem. Pharmacol.* 27:1294–1296.

Janoff, A. S., and K. W. Miller. 1982. A critical assessment of the lipid theories of general anaesthetic action. *In* Biological Membranes. D. Chapman, ed. Academic Press, London. 417–476.

Janoff, A. S., M. J. Pringle, and K. W. Miller. 1981. Correlation of general anesthetic potency with solubility in membranes. *Biochim. Biophys. Acta.* 649:125–128.

Koblin, D., B. Chortkoff, M. Laster, E. Eger, M. Halsey, and P. Ionescu. 1994. Polyhalogenated and perfluorinated compounds that disobey the Meyer-Overton hypothesis. *Anesth. Analg.* 79:1043–1048.

Krasowski, M. D., and N. L. Harrison. 1999. General anaesthetic actions on ligand-gated ion channels. *Cell. Mol. Life Sci.* 55:1278–1303.

Leermakers, F. A. M., and J. Lyklema. 1992. On the self-consistent field theory of surfactaant micelles. *Colloids Surfaces.* 67:239–255.

Leermakers, F. A. M., and J. M. H. M. Scheutjens. 1988. Statistical thermodynamics of association colloids. III. The gel to liquid phase transition of lipid bilayer membranes. *J. Chem. Phys.* 89:6912–6924.

Lindahl, E., and O. Edholm. 2000. Spatial and energetic-entropic decomposition of surface tension in lipid bilayers from molecular dynamics simulations. *J. Chem. Phys.* 113:3882–3893.

Liu, J., M. J. Laster, S. Taheri, E. I. Eger, D. D. Koblin, and M. J. Halsey. 1993. Is there a cutoff in potency for the normal alkanes? *Anesth. Analg.* 77:12–18.

Liu, J., M. J. Laster, D. D. Koblin, E. I. Eger, M. J. Halsey, S. Taheri, and B. Chortkoff. 1994a. A cut-off in potency exists in the perfluoroalkanes. *Anesth. Analg.* 79:238–244.

Liu, J., M. J. Laster, S. Taheri, E. I. Eger, B. Chortkoff, and M. J. Halsey. 1994b. Effect of n-alkane kinetics in rats on potency estimations and the Meyer-Overton hypothesis. *Anesth. Analg.* 79:1049–1055.

Lundbaek, J. A., and O. S. Andersen. 1999. Spring constants for channel-induced lipid bilayer deformations. *Biophys. J.* 76:889–895.

Mascia, M. P., J. R. Trudell, and R. A. Harris. 2000. Specific binding sites for alcohols and anesthetics on ligand-gated ion channels. *Proc. Natl. Acad. Sci. USA.* 97:9305–9310.

Meijer, L. A., F. A. M. Leermakers, and J. Lyklema. 1999. Self-consistent-field modeling of complex molecules with united atom detail in inhomogeneous systems. cyclic and branched foreign molecules in dimyristoylphosphatidylcholine membranes. *J. Chem. Phys.* 110:6560–6579.

Merz, K. M., and B. Roux. 1996. Biological Membranes: A Molecular Perspective from Computation and Experiment. Birkhäuser, Boston.

Meyer, H. H. 1901. Zur Theorie der Alkoholnarkose. Der Einfluss wechselnder Temperature auf Wirkungsstärke und Theilungscoefficient der Narcotica. *Arch. Exp. Pathol. Pharmakol.* 46:338–346.

Meyer, H. H. 1899. Welche eigenschaft der anasthetica bedingt inre Narkotische wirkung? *Arch. Exp. Pathol. Pharmakol.* 42:109–118.

Miller, K. W. 1985. The nature of the site of general anesthesia. *Int. Rev. Neurobiol.* 27:1–61.

Miller, K. W., W. D. M. Paton, R. A. Smith, and E. B. Smith. 1972. Physicochemical approaches to the mode of action of general anesthetics. *Anesthesiology.* 36:339–351.

Morein, S., A.-S. Andersson, L. Rilfors, and G. Lindblom. 1996. Wild type *Escherichia coli* cells regulate the membrane lipid composition in a 'window' between gel and non-lamellar structures. *J. Biol. Chem.* 271: 6801–6809.

Mouritsen, O. G., and M. Bloom. 1993. Models of lipid-protein interactions in membranes. *Annu. Rev. Biophys. Biomol. Struct.* 22:145–171.

Mouritsen, O. G., and K. Jørgensen. 1997. Small-scale lipid-membrane structure: simulation versus experiment. *Curr. Opin. Struc. Biol.* 7:518–527.

Moss, G. W. J., S. Curry, N. P. Franks, and W. R. Lieb. 1991. Mapping the polarity profiles of general anesthetic target sites using *n*-alkane-(α,ω)-diols. *Biochemistry.* 30:10551–10557.

Nielsen, C., M. Goulian, and O. S. Andersen. 1998. Energetics of inclusion-induced bilayer deformations. *Biophys. J.* 74:1966–1983.

North, C., and D. S. Cafiso. 1997. Contrasting membrane localization and behavior of halogenated cyclobutanes that follow or violate the Meyer-Overton hypothesis of general anesthetic potency. *Biophys. J.* 72: 1754–1761.

Overton, C. E. 1901. Studien über die Narkose zugleich ein Beitrag zur allgemeinen Pharmakologie. Gustav Fischer, Jena, Switzerland.

Overton, C. E. 1990. Studies of Narcosis. Chapman and Hall, London.

Popot, J.-L., and D. M. Engelman. 2000. Helical membrane protein folding, stability, and evolution. *Annu. Rev. Biochem.* 69:881–922.

Pratt, M. B., Husain, S. S., Miller, K. W., and J. B. Cohen. 2000. Identification of sites of incorporation in the nicotinic acetylcholine receptor of a photoactivatible general anesthetic. *J. Biol. Chem.* 275: 29441–29451.

Pringle, M. J., Brown, K. B., and K. W. Miller. 1981. Can the lipid theories of anesthesia account for the cutoff in anesthetic potency in homologous series of alcohols? *Mol. Pharmacol.* 19:49–55.

Qin, Z. H., Szabo, G., and D. S. Cafiso. 1995. Anesthetics reduce the magnitude of the membrane dipole potential: measurements in lipid vesicles using voltage sensitive spin probes. *Biochemistry.* 34: 5536–5543.

Seddon, J. M. 1990. Structure of the inverted hexagonal (H_{II}) phase, and non-lamellar phase transitions of lipids. *Biochim. Biophys. Acta.* 1031: 1–69.

Seddon, J. M., and R. H. Templer. 1995. Polymorphism of lipid-water systems. *In* Structure and Dynamics of Membranes. R. Lipowsky and E. Sackmann, eds. Elsevier/North Holland, Amsterdam. 97–160.

Smith, G. D., R. L. Jaffe, and D. Yoon. 1994. Conformational characteristics of poly(tetrafluoroethylene) chains based upon ab initio electronic structure calculations on model molecules. *Macromolecules.* 27: 3166–3173.

Stigter, D., J. Mingins, and K. A. Dill. 1992. Phospholipid interactions in model membrane systems. II. Theory. *Biophys. J.* 61:1616–1629.

Taheri, S., M. J. Halsey, J. Liu, E. I. Eger, D. D. Koblin, and M. J. Laster. 1991. What solvent best represents the site of action of inhaled anesthetics in humans, rats, and dogs? *Anesth. Analg.* 72:627–634.

Tang, P., B. Yan, and Y. Xu. 1997. Different distribution of fluorinated anesthetics and nonanesthetics in model membrane: a 19F NMR study. *Biophys. J.* 72:1676–1682.

Tielemann, D. P., S. J. Marrink, and H. J. C. Berendsen. 1997. A computer perspective of membranes: molecular dynamics studies of lipid bilayer systems. *Biochim. Biophys. Acta.* 1331:235–270.

Ueno, S., J. R. Trudell, E. I. Eger, and R. A. Harris. 1999. Actions of fluorinated alkanols on $GABA_A$ receptors: relevance to theories of narcosis. *Anesth. Analg.* 88:877–883.

Unwin, N. 1993. Nicotinic acetylcholine receptor at 9 Å resolution. *J. Mol. Biol.* 229:1101–1124.

Unwin, N. 1995. Acetylcholine receptor channel imaged in the open state. *Nature.* 373:37–43.

Vaes, W. H. J., E. U. Ramos, C. Hamwijk, I. van Holsteijn, B. J. Blaauboer, W. Seinen, H. J. M. Verhaar, and J. L. M. Hermens. 1997. Solid phase microextraction as a tool to determine membrane/water partition coefficients and bioavailable concentrations in in vitro systems. *Chem. Res. Toxicol.* 10:1067–1072.

Venturoli, M., and B. Smit. 1999. Simulating the self-assembly of model membranes. *Phys. Chem. Comm.* 10.

White, S. H., G. I. King, and J. E. Cain. 1981. Location of hexane in lipid bilayers determined by neutron diffraction. *Nature.* 290:161–163.

Wijmans, C. M., F. A. M. Leermakers, and G. J. Fleer. 1994. Chain stiffness and bond correlations in polymer brushes. *J. Chem. Phys.* 101:8214–8223.

Xiang, T.-X., and B. D. Anderson. 1994. Molecular distributions in interphases: statistical mechanical theory combined with molecular dynamics simulations of a model lipid bilayer. *Biophys. J.* 66:561–573.